

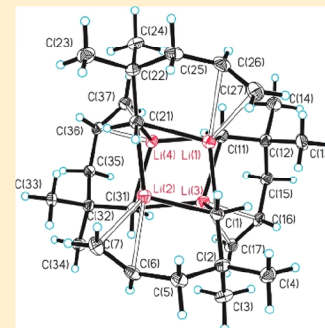
Lithium–Olefin π -Complexes and the Mechanism of Carbolithiation: Synthesis, Solution Behavior, and Crystal Structure of (2,2-Dimethylpent-4-en-1-yl)lithium

Sumeng Liu,¹ Danielle Gray,¹ Lingyang Zhu, and Gregory S. Girolami^{*1,2}

School of Chemical Sciences, University of Illinois at Urbana–Champaign, 600 South Mathews Avenue, Urbana, Illinois 61801, United States

Supporting Information

ABSTRACT: We describe the first crystallographically characterized example of a nonconjugated olefin bound in a simple dihapto fashion to a lithium center, as part of a study of two alkyl lithium compounds that contain C=C double bonds at the alkyl chain terminus: (2,2-dimethylbut-3-en-1-yl)lithium (**1**) and the related pentenyl compound (2,2-dimethylpent-4-en-1-yl)lithium (**2**). The Li–olefin interactions in the crystal structure of **2** serve as a model for those proposed to be present in the [RLi···olefin] intermediate in olefin carbolithiation reactions. As seen in other systems, the Li–olefin interaction is correlated with deshielding of the ¹H NMR resonances of the olefinic hydrogen atoms. DOSY and NOE measurements show that **1** and **2** remain tetrameric in cyclohexane and that the lithium–olefin interactions persist in solution. Addition of a Lewis base such as THF to these ω -alkenyllithium species has two effects: the THF displaces the lithium–olefin interactions while accelerating the rate of carbolithiation. A deuteration experiment shows that compound **2** undergoes reversible carbolithiation to the corresponding cyclobutylmethyl lithium species in the presence of Lewis bases, but this transformation is thermodynamically uphill owing to ring strain. In comparison, the longer chain hexenyl species (2,2-dimethylhex-5-en-1-yl)lithium is thermodynamically unstable with respect to the intramolecular carbolithiation product [(3,3-dimethylcyclopentyl)methyl]lithium (**3**). We suggest that rate-determining step in carbolithiation reactions may not always be formation of the C–C bond, as is often assumed, but in some cases may be formation of the lithium–olefin complex; the coordination of the olefin to lithium may occur in a concerted fashion with disaggregation of lithium clusters. Finally, we point out that activation enthalpies can be obtained solely from NMR line shapes above the coalescence point.



INTRODUCTION

Carbolithiation reactions, in which an organolithium reagent adds across a carbon–carbon double or triple bond to form a new organolithium species, have many uses in synthetic organic chemistry.^{1–5} In such carbolithiation reactions, the addition step is immediately preceded by formation of an intermediate in which there is a direct lithium–olefin interaction;^{4,6–17} the structure of this intermediate is thought to be principally responsible for the chemo-, regio-, and stereoselectivity of the addition step.^{8,10,13–15,17,18} Computational studies support this view: the intermolecular reaction between methyl lithium and ethylene occurs through initial formation of a Li–ethylene π -complex, followed by syn-addition of methyl lithium across the carbon–carbon double bond.¹⁹ Theoretical studies have shown that intermediates with similar lithium–olefin interactions are also crucial for the steric control of intramolecular carbolithiation reactions.^{15,20}

The experimental study of lithium–olefin interactions involving alkyl lithium reagents is challenging:^{1,13} in ether solvents, simple olefins such as ethylene insert rapidly into the Li–C bond of alkyl lithium reagents even at -50°C .²¹ One approach is to study such interactions at low temperatures by techniques such as ¹H–⁶Li HOSEY²² and resonance Raman¹⁴

spectroscopy. Another approach is to disfavor insertion of the olefin into the Li–C bond, for example, by employing ω -alkenyllithium species with five or fewer carbon atoms in the chain (for which the open-ring form is thermodynamically more stable owing to the ring strain of the cyclized reaction product),²³ or by carrying out the studies in hydrocarbon rather than ether solvents.²⁴ Thus, IR and ¹H NMR studies of 3-butenyllithium in hydrocarbon solvents found that Li–olefin interactions cause the C=C stretching frequency to decrease by 6 cm^{-1} , and the olefinic protons to be deshielded with respect to the corresponding hydrocarbon 1-butene.^{25,26} In contrast, in diethyl ether, the olefinic protons are shielded compared to 1-butene as expected from inductive effects.

Crystallographically characterized compounds in which lithium interacts with conjugated olefins are well-known,^{11,27–29} but there are remarkably few examples of crystal structures in which a lithium cation is coordinated to a nonconjugated olefin. In the few reported examples of such species, the lithium–olefin interactions are almost always accompanied by other types of interactions. For example, the

Received: March 13, 2019

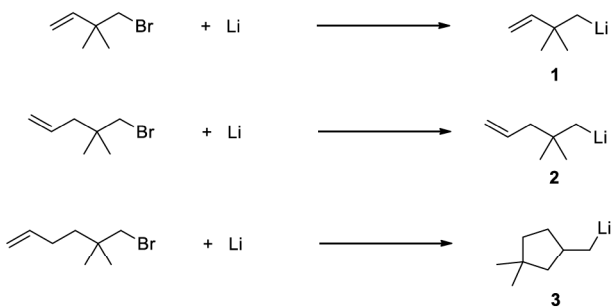
Published: April 29, 2019

olefin is often π -bonded to an anionic transition metal center,^{11,28,30} so that the Li–olefin interaction is enhanced by attractive electrostatic forces. There are two crystal structures of compounds that exhibit short lithium–carbon contacts to a nonconjugated and otherwise noncoordinated olefin.^{31,32} In both compounds, the lithium cations are principally interacting with negative charges (allyl or carborane anions) located adjacent to the olefins. Because the linkages between the olefins and the anions in these compounds are conformationally inflexible, the olefins are close to the lithium cations for a simple reason: they have to be.

We now describe the synthesis and characterization of two ω -alkenyllithium compounds that contain lithium–olefin π -interactions. To the best of our knowledge, our crystal structure of (2,2-dimethylpent-4-en-1-yl)lithium is the first in which lithium is coordinated to a nonconjugated olefin in the absence of other complicating interactions or conformational constraints. This crystal structure serves as an informative structural model of the key intermediate in carbolithiation reactions. We also report NMR studies that suggest that the solid state structure, including the Li–olefin interactions, is maintained in hydrocarbon solution. Finally, we assess the strength of this interaction and discuss the possible relevance of these results to the mechanism of carbolithiation reactions.

RESULTS AND DISCUSSION

Synthesis of the ω -Alkenyllithium Species $\text{LiCH}_2\text{CMe}_2\text{CH}=\text{CH}_2$ and $\text{LiCH}_2\text{CMe}_2\text{CH}_2\text{CH}=\text{CH}_2$. Treatment of 4-bromo-3,3-dimethyl-1-butene with excess lithium in pentane/diethyl ether affords the new ω -alkenyllithium species (2,2-dimethylbut-3-en-1-yl)lithium (**1**), which can be isolated as a light yellow oil with a melting point of below -20°C .



Similar treatment of 5-bromo-4,4-dimethyl-1-pentene with excess lithium in 1:1 (v/v) pentane/diethyl ether, followed by evaporation of the solvent and crystallization from pentane, affords colorless crystals of (2,2-dimethylpent-4-en-1-yl)lithium (**2**). These crystals can be stored indefinitely under argon at -20°C , and pentane solutions of both **1** and **2** can be stored under argon at -20°C for months without decomposition.

Attempts to make the analogous compound with six carbon atoms in the alkyl backbone (instead of four or five) by lithiation of 6-bromo-5,5-dimethyl-1-hexene under similar conditions do not afford (2,2-dimethylhex-5-en-1-yl)lithium, but instead lead to an organolithium product that shows no olefinic signals in its ^1H NMR spectrum. This product has been identified as [(3,3-dimethylcyclopentyl)methyl]lithium (**3**), which is the result of an intramolecular carbolithiation reaction. The formation of this compound is consistent with previous reports that hex-5-en-1-yl lithium compounds cyclize

to (cyclopentylmethyl)lithium derivatives in pentane–diethyl ether solvents.⁴

The ^1H NMR spectrum of the substituted butenyllithium compound **1** contains a singlet at δ -0.80 assigned to the anionic $\alpha\text{-CH}_2$ group; such shielded chemical shifts are typically seen for protons attached to the anionic center in organolithium reagents.³³ More interestingly, the chemical shift of the methine proton attached to the C=C double bond is deshielded by ~ 0.3 ppm compared to the chemical shift of the analogous proton in the conjugate acid of this anion, 3,3-dimethyl-1-butene. Similar deshielding of olefinic protons is also seen in 3-butenyllithium^{25,26} and several alkenylaluminum reagents.^{34,35} This deshielding is the opposite of what would be expected based on inductive effects; consistent with these earlier studies, we believe that it reflects the proximity of the olefin to the Lewis acidic lithium center. The ^{13}C NMR and ^7Li NMR spectra of **1** are similar to those of **2**, which will be discussed in detail next.

The ^1H NMR spectrum of the substituted pentenyllithium compound **2** at 20°C in cyclohexane- d_{12} (C_6D_{12}) shows a broad singlet (fwhm = 6.45 Hz) at δ -0.83 assigned to the anionic $\alpha\text{-CH}_2$ group (the large line width is likely due to unresolved coupling to ^6Li or ^7Li). The methine proton attached to the C=C double bond appears as a multiplet at δ 6.19 ; again, its chemical shift is deshielded by 0.4 ppm compared to that of the methine proton in the corresponding conjugate acid, 4,4-dimethyl-1-pentene (δ 5.78 in C_6D_{12}). The olefinic CH_2 , $\gamma\text{-CH}_2$, and $\beta\text{-methyl}$ proton signals are also deshielded with respect to the unlithiated alkene, but to a lesser extent: the olefinic CH_2 protons are at δ 5.11 and 5.17 (vs δ 4.95), the $\gamma\text{-CH}_2$ protons are at δ 2.04 (vs δ 1.92), and the $\beta\text{-methyl}$ protons are at δ 1.06 (vs δ 0.89). Similar deshielding of these protons is also seen for solutions of **2** in the aromatic solvent C_6D_6 (see SI).

The IR spectrum of **2** features a C=C stretch at 1628 cm^{-1} that is 13 cm^{-1} lower than the 1641 cm^{-1} frequency seen for its conjugate acid 4,4-dimethyl-1-pentene.³⁶ This observation is consistent with previous infrared and resonance Raman studies of lithium–olefin complexes.^{14,25,26} However, the lowered C=C stretching frequency is not definitive evidence of the presence of a Li–olefin interaction because this mode can be affected by other factors such as coupling to other vibrations, strain, and inductive effects.³⁷

The ^7Li NMR spectrum of **2** in cyclohexane- d_{12} consists of a singlet at δ 2.01. The ^{13}C signal of the $\alpha\text{-CH}_2$ group appears as a broad peak at δ 32.8; unresolved ^{13}C – $^{6,7}\text{Li}$ coupling may be present. These ^7Li NMR³⁸ and ^{13}C NMR³⁹ shifts are similar to those seen in other alkylolithium compounds.

Crystal Structure of $\text{LiCH}_2\text{CMe}_2\text{CH}_2\text{CH}=\text{CH}_2$ (2). Crystal data for the 2,2-dimethylpentenyl compound **2** are presented in Table 1, and selected bond length and angles are collected in Table 2. In the solid state, this compound exists as an unsolvated tetramer in which the four lithium atoms form a distorted tetrahedron (Figure 1). As usual, each face of the tetrahedron is capped by one of the anionic $\alpha\text{-CH}_2$ groups.⁴⁰ Interestingly, of the five largest peaks in the final difference map for **2**, four were located just under 1 \AA away from the four α -carbon atoms, along lines that connect those carbon atoms with the center of the Li_4 tetrahedron. These four electron density features are assigned to the lone pairs on each of the anionic α -carbon atoms.

Overall, the (2,2-dimethylpent-4-en-1-yl)lithium tetramer has idealized (but not crystallographic) $\bar{4}$ symmetry, in which

Table 1. Crystallographic Data for (2,2-Dimethylpent-4-en-1-yl)lithium (2)

| space gp, $P\bar{1}$ | formula, $C_{28}H_{52}Li_4$ |
|---|--|
| $T = 100$ K | $FW = 416.45$ g/mol |
| $\lambda = 0.71073$ Å | $V = 1501.94(9)$ Å ³ |
| $a = 9.5665(3)$ Å | $Z = 2$ |
| $b = 11.7202(4)$ Å | $\rho_{\text{calc}} = 0.921$ g/cm ³ |
| $c = 13.9363(5)$ Å | $\mu = 0.048$ mm ⁻¹ |
| $\alpha = 88.0409(10)^\circ$ | $R_{\text{int}} = 0.036$ |
| $\beta = 74.6859(10)^\circ$ | $\text{GOF on } F^2 = 1.038$ |
| $\gamma = 85.3298(10)^\circ$ | |
| absorption correction: face-indexed | |
| max, min transm. factors: 1.00, 0.97 | |
| data, parameters, restraints: 5504, 0, 358 | |
| $R_1 [I > 2\sigma(I)]^a = 0.0558$; wR_2 (all data) ^b = 0.1434 | |
| max, min $\Delta\rho_{\text{electron}} = 0.77$, -0.21 e/Å ³ | |
| ^a $R_1 = \sum F_0 - F_c / \sum F_0 $. ^b $wR_2 = [\sum w(F_0^2 - F_c^2)^2 / \sum (F_0^2)^2]^{1/2}$. | |

Table 2. Selected Bond Distances and Angles for (2,2-Dimethylpent-4-en-1-yl)lithium (2)

| bond distances (Å) | | | |
|--------------------|------------|---------------|------------|
| Li1—C1 | 2.221(3) | Li3—C1 | 2.268(3) |
| Li1—C11 | 2.272(3) | Li3—C11 | 2.244(3) |
| Li1—C21 | 2.246(3) | Li3—C31 | 2.274(3) |
| Li1—C26 | 2.491(3) | Li3—C16 | 2.425(3) |
| Li1—C27 | 2.536(3) | Li3—C17 | 2.593(3) |
| Li2—C1 | 2.245(3) | Li4—C11 | 2.260(3) |
| Li2—C21 | 2.233(3) | Li4—C21 | 2.268(3) |
| Li2—C31 | 2.257(3) | Li4—C31 | 2.236(3) |
| Li2—C6 | 2.494(3) | Li4—C36 | 2.425(3) |
| Li2—C7 | 2.490(3) | Li4—C37 | 2.599(3) |
| C6—C7 | 1.323(3) | C26—C27 | 1.324(3) |
| C16—C17 | 1.318(3) | C36—C37 | 1.322(3) |
| bond angles (deg) | | | |
| C26—Li1—C27 | 30.53(8) | C16—Li3—C17 | 30.22(7) |
| C27—C26—Li1 | 76.60(13) | C17—C16—Li3 | 81.99(12) |
| C26—C27—Li1 | 72.87(13) | C16—C17—Li3 | 67.80(11) |
| C7—Li2—C6 | 30.79(7) | C36—Li4—C37 | 30.24(6) |
| C7—C6—Li2 | 74.45(12) | C37—C36—Li4 | 82.19(12) |
| C6—C7—Li2 | 74.76(12) | C36—C37—Li4 | 67.57(11) |
| C7—C6—C5 | 125.87(17) | C27—C26—C25 | 126.0(2) |
| C7—C6—H6 | 119.4(12) | C27—C26—H26 | 117.7(13) |
| C5—C6—H6 | 114.7(12) | C25—C26—H26 | 116.2(13) |
| C6—C7—H7A | 121.1(13) | C26—C27—H27B | 118.6(14) |
| C6—C7—H7B | 121.8(12) | C26—C27—H27A | 118.3(13) |
| H7A—C7—H7B | 117.0(18) | H27B—C27—H27A | 123.1(19) |
| C17—C16—C15 | 125.12(17) | C37—C36—C35 | 125.38(16) |
| C17—C16—H16 | 119.5(12) | C37—C36—H36 | 117.1(11) |
| C15—C16—H16 | 115.4(11) | C35—C36—H36 | 117.5(11) |
| C16—C17—H17A | 120.9(13) | C36—C37—H37A | 121.1(12) |
| C16—C17—H17B | 122.7(12) | C36—C37—H37B | 121.8(12) |
| H17A—C17—H17B | 116.4(17) | H37A—C37—H37B | 117.1(17) |

each of the ω -alkenyl chains is approximately perpendicular to the $\bar{4}$ axis. The structure of **2** is analogous to that of the 3-lithio-1-methoxybutane tetramer,⁴¹ but is different from those of the 1-dimethylamino-3-lithiopropane⁴² and 1-lithio-3-methoxypropane⁴³ tetramers, in which the bidentate chains lie approximately parallel to the $\bar{4}$ axis.

The most interesting structural feature in **2** is the η^2 coordination of each of the $C=C$ double bonds at the ends

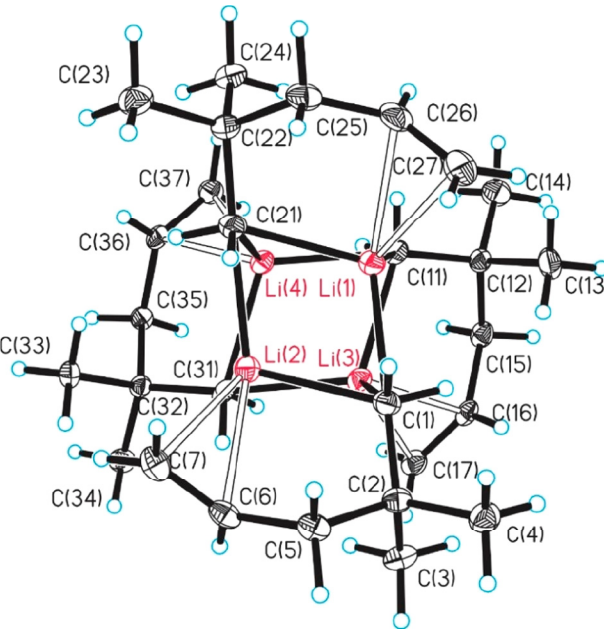


Figure 1. Crystal structure of (2,2-dimethylpent-4-en-1-yl)lithium (2), viewed down the noncrystallographic molecular $\bar{4}$ axis. Ellipsoids are drawn at the 35% probability level.

of the ω -alkenyl chains to a different lithium atom in the tetramer. The average Li—C distances to the olefinic methine and methylene carbons of 2.46(2) and 2.55(3) Å, respectively, are longer than the 2.01 Å sum of the covalent radii of lithium (1.28 Å) and an sp^2 carbon (0.73 Å),⁴⁴ but are considerably shorter than the 3.51 Å sum of the van der Waals radii for lithium (1.81 Å) and an sp^2 carbon (1.70 Å).⁴⁵ The Li—C(olefin) distances in **2** can be compared with those in the conformationally constrained compounds mentioned earlier: they are shorter than the Li—C distances of 2.60 Å in $[\text{Li}_4(\text{THF})_5[1,2\text{-}(\text{CH}_2\text{CH}=\text{CHCH}_2)\text{-}1,2\text{-C}_2\text{B}_{10}\text{H}_{10}]]_2$, but longer than those of 2.40 and 2.43 Å in bicyclo[3.2.1]octa-2,6-dienyllithium.^{31,32}

The average C=C double bond length of 1.322(2) Å in **2** is very close to those of 1.32 Å seen in free olefins,⁴⁶ and those of 1.32 to 1.36 Å in olefins bound to calcium,⁴⁷ barium,⁴⁷ aluminum,⁴⁸ and d⁰ zirconium centers.⁴⁹ In addition, we were able to locate all the olefinic hydrogens in the difference map and to refine their locations without constraints. The olefinic carbon atoms in **2** are planar within error, and are not pyramidalized as seen in olefin complexes of d¹–d¹⁰ transition metal centers in which there is metal to ligand π -backbonding.

The 2.46(2)–2.55(3) Å Li—C(olefin) distances and the 1.322(2) Å C=C distance in **2** are in good agreement with those computed for of an ethylene–methylolithium complex in which the ethylene binds to lithium in an η^2 mode.¹⁹ The optimized Li—C(olefin) distance in the computational study was 2.544 Å, and the optimized C=C double bond length was 1.325 Å. The Li–olefin interaction energy was calculated to be ~ 12 kcal/mol. The experimental Li—C bond length in **2** is slightly longer than those in another computational study, which found Li—C distances of 2.407 and 2.380 Å in the chairlike ground state structure of 5-hexen-1-yllithium.¹⁵ We point out, however, that both of these computations were carried out on monomeric alkylolithium species, not a tetrameric structure as we see for **2**.

DOSY and 1D NOE Studies of 1 and 2 in Solution. In this section, we describe NMR studies to address two questions: (1) Is the tetrameric structure seen in the solid-state preserved in solution? (2) Are the Li–olefin interactions seen in the solid-state preserved in solution?

To determine the degree of oligomerization of **1** and **2** in solution, we carried out ^1H diffusion-ordered spectroscopy (DOSY) experiments in C_6D_{12} at 25 °C using adamantane as the internal standard (Figure 2).^{50,51}

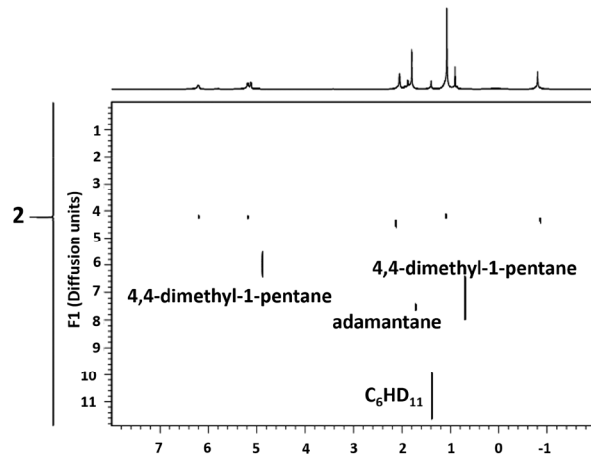


Figure 2. ^1H DOSY spectrum of **2** in cyclohexane- d_{12} at 25 °C.

For the dimethylbutenyl compound **1**, the ^1H NMR diffusivity is $(4.54 \pm 0.05) \times 10^{-10} \text{ m}^2/\text{s}$ (essentially identical diffusivities were deduced from each of the different proton environments); this diffusivity corresponds to a molecular weight of 410 ± 60 vs a calculated value of 360 for tetrameric **1**. Similarly, for the dimethylpentenyl compound **2**, all five ^1H NMR resonances exhibit the same diffusivity (averaging $(4.3 \pm 0.1) \times 10^{-10} \text{ m}^2/\text{s}$). This value corresponds to a molecular weight of 450 ± 65 (see [Experimental Section](#)), which is consistent with the calculated molecular weight of 416 for tetrameric **2**.

Diffusion coefficients are sensitive to the shape and the hydrodynamic radius of the particle, and the latter is related to the volume of the molecule.⁵⁰ Because our organolithium compounds are somewhat less dense (as judged from the crystal structure) than the calibration standard adamantane (e.g., 0.92 g/cm³ for **2** vs 1.08 g/cm³ for adamantane⁵²), the DOSY measurements are likely to give slight overestimates of the molecular weights of the organolithium compounds. As a result, our measurements are consistent with the conclusion that, for **1** and **2**, the dominant species in C_6D_{12} solution are tetramers, and not hexamers as seen for certain alkylolithium species such as *n*-butyllithium,^{53,54} isopropyllithium,^{53,54} cyclohexyllithium,^{53,54} and cyclopentyllithium.⁵⁵

To determine whether the lithium–olefin contacts observed in the crystal structure of **2** persist in solution, we measured the heteronuclear $^1\text{H}\{^7\text{Li}\}$ nuclear Overhauser enhancements (NOEs) at 25 °C in C_6D_{12} . Absolute heteronuclear NOEs are difficult to measure directly because they are small. The largest NOE is expected for the $\alpha\text{-CH}_2$ protons (which are certainly in proximity to the Li centers); we find that the absolute NOE for these protons is $3 \pm 1\%$. By subtracting the normal ^1H NMR spectrum from one in which the ^7Li resonance is saturated, the relative NOEs for different protons

can be measured fairly accurately. If the intensity of the $\alpha\text{-CH}_2$ protons in this difference spectrum is set arbitrarily to 1.00, the relative intensities of the NOE difference peaks for the protons in the chain are Li–CH₂(1.0)–CMe₂–CH₂(0.03)–CH(0.17)=CH₂(0.16) (Figure 3). These intensities correspond to absolute NOEs (after correcting for the site populations) of Li–CH₂(3%)–CMe₂–CH₂(0.1%)–CH(1.0%)=CH₂(0.5%).

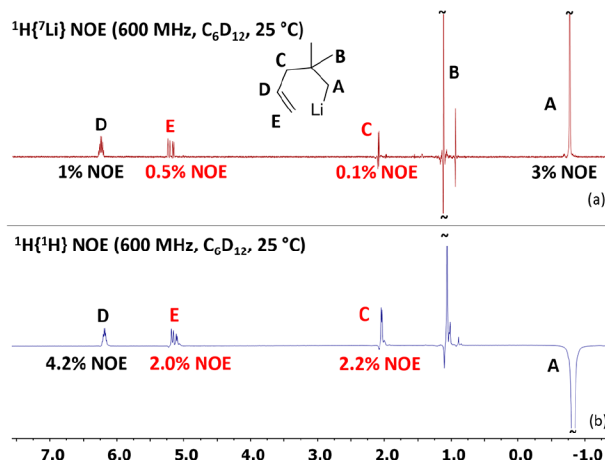


Figure 3. (a) Difference spectrum showing relative heteronuclear $^1\text{H}\{^7\text{Li}\}$ nuclear Overhauser enhancements (NOEs) of **2** in cyclohexane- d_{12} at 25 °C. (b) 1D homonuclear $^1\text{H}\{^1\text{H}\}$ NOE NMR spectrum of **2** in cyclohexane- d_{12} at 25 °C. The $\alpha\text{-CH}_2$ resonance (A) is irradiated for 2 s.

Thus, the olefinic protons have $^1\text{H}\{^7\text{Li}\}$ NOEs that are 5 to 10 times larger than seen for the $\gamma\text{-CH}_2$ protons (although smaller than those seen for the lithium-bound $\alpha\text{-CH}_2$ protons). These $^1\text{H}\{^7\text{Li}\}$ NOEs suggest that, in hydrocarbon solution, the olefinic protons of **2** are closer than the $\gamma\text{-CH}_2$ protons to the lithium atom, despite being at the end of the ω -alkenyl chain. The relative sizes of these NOEs are consistent with the crystal structure of **2**, in which the shortest Li–H distances are to the $\alpha\text{-CH}_2$ protons ($\sim 2.1 \text{ \AA}$), the next shortest are to the olefinic methine and methylene protons (~ 2.7 and 2.8 \AA , respectively), and all other Li–H distances are longer than 3.1 \AA .

Lithium–olefin interactions also persist in solutions of the dimethylbutenyl compound **1**, as shown by its $^1\text{H}\{^7\text{Li}\}$ difference NOE spectrum at 25 °C (see [Supporting Information \(SI\)](#)). The absolute NOEs for the olefinic methylene and methine protons ($0.3 \pm 0.1\%$ and $1 \pm 0.5\%$, respectively) are very similar to those in **2**; these results again indicate that the olefin group is in close proximity to lithium.

Finally, a homonuclear $^1\text{H}\{^1\text{H}\}$ NOE study in C_6D_{12} at 25 °C provides additional evidence that the olefinic methylene protons of **2** are close to the $\alpha\text{-CH}_2$ protons (Figure 3): when the $\alpha\text{-CH}_2$ peak at $\delta = 0.83$ is irradiated for 2 s, the NOE of the terminal olefinic methylene protons (2.0%) is similar in size to that of the $\gamma\text{-CH}_2$ protons (2.2%). This result is consistent with the conformation of the 2,2-dimethylpent-4-en-1-yl ligand observed in the crystal structure of **2**, in which the $\gamma\text{-CH}_2$ protons and the olefinic methylene protons are approximately equidistant from the $\alpha\text{-CH}_2$ protons.

All these findings strongly suggest that, when **1** and **2** are dissolved in cyclohexane, they exist as tetramers in which the

$\text{C}=\text{C}$ double bond is coordinated to the lithium center, as seen in the solid state.

Strength of the Li–Olefin Interaction. In the crystal structure of **2**, the coordination of the lithium to one side of the $\text{C}=\text{C}$ double bond lowers the symmetry in such a way that the two β -methyl groups in each ω -alkenyl chain are in chemically inequivalent environments (as are the two protons of the allylic γ -methylene group).⁵⁶ The ^1H NMR spectrum of **2** at room temperature, however, shows that the two diastereotopic β -methyl groups are equivalent on the NMR time scale; exchange of the two β -methyl environments can occur only if the olefin dissociates and then reassociates via the other face of the $\text{C}=\text{C}$ double bond.⁴⁹ Other processes, such as intramolecular isomerization between the two types of **4** structures,⁴² do not exchange these sites.

A variable temperature ^1H NMR study of **2** in C_7D_{14} showed that when the sample is cooled from -10 to -80 °C the methyl resonance broadens by ~ 6 Hz (from 4.3 to 10.7 Hz) and the $\alpha\text{-CH}_2$ resonance broadens by a similar amount, ~ 5 Hz. In contrast, when the sample is cooled from -10 to -80 °C the peaks due to the olefinic protons of **2**, and those due to the methyl groups of the hydrolysis product 4,4-dimethyl-1-pentene, broaden by only ~ 1.6 Hz; this small broadening probably reflects decreases in relaxation times due to increased solvent viscosity and/or instrumental effects such as changes in shimming. Therefore, the much more pronounced broadening of the methyl resonance in **2** at -80 °C is most likely a sign of incipient decoalescence due to slowing of the exchange process. From the amount of line broadening, we can estimate the enthalpy of activation for the dissociation of the $\text{C}=\text{C}$ bond in **2** to be ~ 3 kcal/mol (see **Experimental Section**). This value provides a lower limit for the strength of the Li–olefin interaction; the bond strength will be higher if solvent participates in the dissociation process^{57,58} or some ring strain is relieved upon dissociation.

Another way to evaluate the strength of the Li–olefin interaction is to determine how easily this interaction can be disrupted by addition of ethers. A solution of **2** in methylcyclohexane- d_{14} (C_7D_{14}) was treated with 2.5 equiv per tetramer of diethyl ether at -38.1 °C. For this solution, we find the following: (1) The chemical shifts of the olefinic protons are still deshielded compared to those in the corresponding conjugate acid; (2) in the difference $^1\text{H}\{^7\text{Li}\}$ NOE spectrum, the relative NOEs (scaled by setting the NOE for the $\alpha\text{-CH}_2$ protons to 1.00) are essentially identical to those seen for an ether-free sample (see **SI**); (3) in the $^1\text{H}\{^1\text{H}\}$ NOE spectrum obtained upon irradiation of the $\alpha\text{-CH}_2$ protons, the NOEs for the olefinic methylene protons (1.0%) are about the same size as the NOE for the $\gamma\text{-CH}_2$ protons (1.2%) (**Figure 4**); and (4) in the ^7Li NMR spectrum at room temperature, the chemical shift of **2** in the presence of diethyl ether (δ 1.67) is similar to the chemical shift of **2** (δ 2.01) in the absence of diethyl ether. All this evidence strongly suggests that the $\text{C}=\text{C}$ double bond in **2** remains coordinated to lithium even in the presence of small amounts of diethyl ether.

In contrast, addition of 16 equiv of THF per tetramer to a C_7D_{14} solution of **2** at -38.1 °C results in significant disruption of the Li–olefin interactions, as shown by the following evidence: (1) the deshielding of the olefinic protons that signals the presence of Li–olefin interactions is significantly smaller. Relative to the ^1H NMR chemical shifts of the conjugate acid 4,4-dimethyl-1-pentene, addition of THF

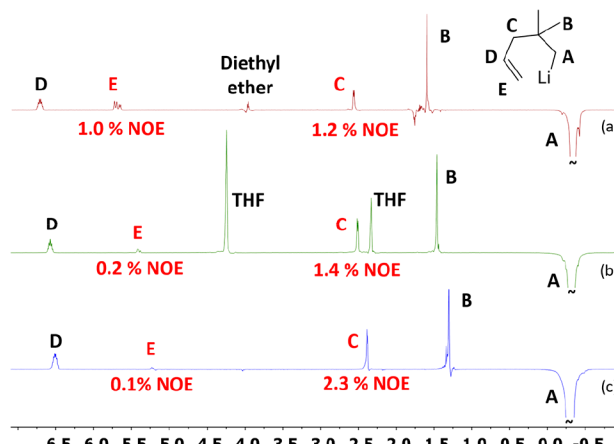


Figure 4. $^1\text{H}\{^1\text{H}\}$ NMR spectra at -38.1 °C showing NOEs of the olefinic CH_2 protons (E) and $\gamma\text{-CH}_2$ protons (C) of **2**, obtained upon irradiation of the $\alpha\text{-CH}_2$ protons (A) under the following conditions: (a) in C_7D_{14} with ~ 2.5 equiv per tetramer of diethyl ether; (b) in C_7D_{14} with ~ 16 equiv per tetramer of THF; (c) in neat $\text{THF-}d_8$.

causes the deshielding of the olefinic methine proton to decrease from 0.41 to 0.25 ppm; furthermore, the olefinic methylene protons are no longer deshielded relative to the conjugate acid but instead are *shielded* by ~ 0.1 ppm; (2) in the difference $^1\text{H}\{^7\text{Li}\}$ NOE spectrum, the NOEs for the olefinic protons decrease by about a factor of 4 so that they are approximately the same as the NOE for the $\gamma\text{-CH}_2$ protons, vs 5 to 10 times larger in the absence of THF; (3) irradiation of the $\alpha\text{-CH}_2$ peak for 2 s gives a $^1\text{H}\{^1\text{H}\}$ NOE of only 0.2% for the terminal olefinic CH_2 protons and 1.4% for the $\gamma\text{-CH}_2$ protons (**Figure 4**), whereas in the absence of THF these NOEs are approximately equal; (4) the ^7Li NMR spectrum of **2** in the presence of 16 equiv of THF per tetramer shows a singlet at δ 2.71, which differs from the ^7Li NMR chemical shift of δ 1.67 seen for **2** in the presence of diethyl ether; and (5) in the difference $^1\text{H}\{^7\text{Li}\}$ NOE spectrum, the 2- CH_2 resonances of THF show a significant NOE (for comparison, upon addition of 2.5 equiv of diethyl ether per tetramer, the 1- CH_2 resonance of diethyl ether shows a negligible NOE). All these findings are consistent with the conclusion that, upon addition of 16 equiv of THF per tetramer, more than half of the Li–olefin interactions have been replaced by Li–THF interactions.

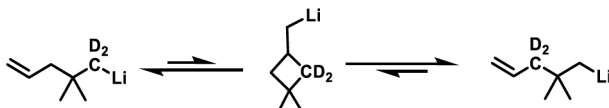
The Li–THF bond enthalpy of sterically hindered alkylolithium compounds in benzene is ~ 10 kcal/mol.^{56,59} This value, which places an upper limit on the strength of the Li–olefin interaction in **2**, is consistent with our estimation from the NMR line broadening analysis that ΔH for the Li–olefin interaction is not less than $\sim 3 \pm 1$ kcal/mol.

We will not discuss the results in detail here, but dissolving **2** in $\text{THF-}d_8$ causes changes in the chemical shifts and NOEs that are consistent with complete loss of the Li–olefin interactions (**Figure 4**).

Reversible Carbolithiation of 2. As noted above, efforts to prepare the hexenyllithium compound (2,2-dimethylhex-5-en-1-yl)lithium led instead to the carbolithiated product [(3,3-dimethylcyclopentyl)methyl]lithium (**3**). This result prompted us to examine whether **2** can undergo reversible carbolithiation, as has been seen previously for other pentenyllithium and Grignard reagents, including $\text{LiCH}(\text{Me})\text{CH}_2\text{CH}_2\text{CH}=\text{CH}_2$ ²³ and $\text{ClMgCH}_2\text{CH}_2\text{CH}_2\text{CH}=\text{CH}_2$.⁶⁰ According to Baldwin's rules, such exo-trig cyclization reactions should have relatively

low barriers (although they may still be uphill thermodynamically) for 3-butenyl, 4-pentenyl, and 5-hexenyllithium reagents.^{61,62}

An excellent way to determine whether reversible carbolithiation is taking place is to deuterate the α -CH₂ protons. If reversible intramolecular carbolithiation occurs, these deuterium labels should scramble into the allylic γ -CH₂ groups:



We found that treatment of BrCD₂CMe₂CH₂CH=CH₂ (>95% deuterated at the indicated site) with lithium in 1:1 diethyl ether/pentane at -20°C for 5 h gives an organolithium reagent that consists of \sim 87% 2- α -d₂ and \sim 13% of LiCH₂CMe₂CD₂CH=CH₂ (2- γ -d₂) as judged from the ¹H NMR spectrum. This result shows that some scrambling has occurred. If the \sim 87% 2- α -d₂ and \sim 13% 2- γ -d₂ mixture is purified and then dissolved in pentane, no further change in the α -d₂ vs γ -d₂ ratio takes place at -20°C even after 7 days. If, however, the mixture is dissolved in 1:1 diethyl ether/pentane and kept at -20°C for 7 days, the exchange reaction reaches equilibrium to afford a 50%/50% mixture of the 2- α -d₂ and 2- γ -d₂ isotopologs.

This evidence shows four things: (1) In the presence of ether, **2** can undergo reversible carbolithiation. (2) The cyclobutylmethyl intermediate responsible for the exchange process in **2** is not directly observable because the strain energy associated with its cyclobutane ring disfavors it thermodynamically (by about 6.4 kcal/mol)⁶³ with respect to the open-chain pentenyl structure. (3) The presence of a lithium–olefin interaction is not sufficient for carbolithiation to occur because in hydrocarbon solvents (where this interaction is present) the rate is very slow. (4) Carbolithiation is accelerated in coordinating solvents, which suggests that a Lewis base is coordinated to the intermediate responsible for carbolithiation. The last of these conclusions is consistent with previous observations of inter- and intramolecular carbolithiation reactions.^{15,19,24,64,65}

Solvation of the lithium centers by a Lewis base can have several chemical consequences, one of which is disaggregation of the organolithium cluster.^{1,5,40,66–68} In fact, Mattalia et al. have proposed that disaggregation is largely responsible for the increased rate of carbolithiation in the presence of Lewis bases.⁹ We comment here that it makes sense that solvation-induced disaggregation should increase the nucleophilicity of the anionic carbon center, for two reasons. First, disaggregation will result in the anionic carbon being bound to fewer positively charged lithium ions. Second, the crystal structure of **2** shows that the lone pairs on the α carbon are pointing to the center of the Li₄ cluster, which is not a favored geometry for the exo-trig cyclization reaction according to Baldwin's rules.^{61,62} Thus, the acceleration of carbolithiation reactions by Lewis bases may reflect a solvation-promoted change in how the anionic carbon binds to lithium, so that the carbanionic lone pair adopts a geometry more favorable for forming a C–C bond with the olefin.¹⁹

Mechanism of Carbolithiation. We briefly consider here the question of the rate-determining step in carbolithiation reactions.^{4,6–17} Carbolithiation reactions are thought to proceed through a monomeric (i.e., Lewis-base-coordinated)

lithium species in which the anionic carbon and the olefin are simultaneously bound to lithium.^{9,20} Although ab initio studies of gas phase carbolithiation reactions have suggested that coordination of the olefin to lithium is downhill thermodynamically by 12 kcal/mol,^{15,19} these calculations involved unsolvated organolithium monomers, which are quite different from the species actually present in solution. Our studies suggest that, in THF, which is a common solvent for carbolithiation reactions, the dominant species in solution before carbolithiation occurs are ones in which no Li–olefin interactions are present. As a result, the formation of lithium–olefin interactions in the presence of excess THF must be uphill thermodynamically. This conclusion is consistent with our finding that the Li–olefin bond strength in **2** is slightly larger than 3 kcal/mol, vs the Li–THF bond strength of about 10 kcal/mol seen for a representative organolithium species, 3-lithio-1-methoxybutane.⁵⁶

Thus, the mechanism of carbolithiation must involve at least two energy barriers: one for formation of the monomeric lithium–olefin complex, and one for the C–C bond formation step (Figure 5). Although it has often been assumed that C–C

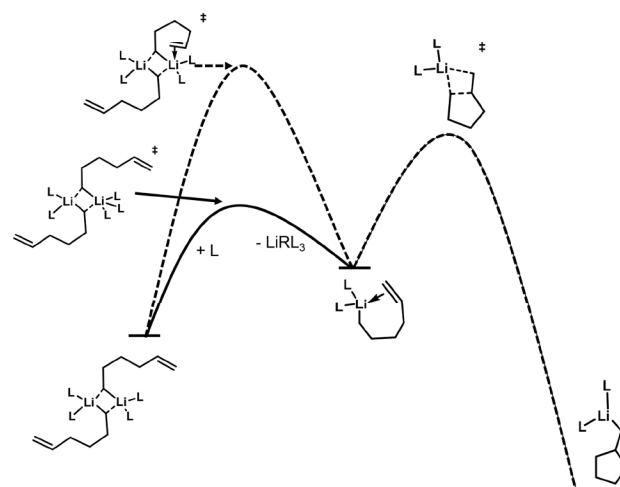


Figure 5. Reaction coordinate for intramolecular carbolithiation reactions. Solid line: reaction coordinate when C–C bond formation step is rate determining, characterized by fast cluster disaggregation promoted by a Lewis base. Dashed line: reaction coordinate when olefin coordination is rate determining, characterized by slow cluster disaggregation induced by olefin coordination.

bond formation has the higher energy barrier, we wish to suggest that coordination of olefin to the solvated lithium center (which may also promote disaggregation of lithium clusters) may have the higher barrier in some systems. Coordination of substrate is known to be rate-determining in other reactions that involve highly reactive metal centers and low-reactivity substrates, such as the activation of C–H bonds in hydrocarbons by some platinum complexes.^{69–71}

Several computational studies (mostly by ab initio methods) have been carried out to estimate the activation energy for the C–C bond forming step in carbolithiation reactions.^{9,15,19,20} The most chemically relevant of these calculations, which involved a THF-solvated organolithium monomer with the olefin already coordinated to the lithium center, gave activation energies for the C–C bond forming step of only 5–15 kcal/mol.^{9,20} Such low barriers suggest that the C–C bond forming step may not be rate determining, particularly if the formation

of a monomeric lithium–olefin complex intermediate is sufficiently inhibited.

Additional evidence that C–C bond formation is not rate determining in some carbolithiation reactions comes from a study of 2-(N-allyl-N-benzylamino)phenyllithium vs its *N*-3-phenenyl analog in toluene with (–)-sparteine as a chiral auxiliary: calculations suggested that the 3-phenenyl compound should have a much lower barrier for the C–C bond forming step,⁹ whereas experimentally the 3-phenenyl compound requires a significantly higher temperature for the carbolithiation reaction to proceed.⁷² A reasonable way to explain this discrepancy is that olefin coordination is rate determining (being hindered by the increased steric bulk of 3-phenenyl vs allyl) instead of C–C bond formation.

The coordination of olefin may occur in a concerted fashion with cluster disaggregation to form monomeric species (i.e., coordination may actually induce disaggregation): even bases that interact weakly with lithium can markedly accelerate cluster disaggregation processes.⁷³ Thus, olefin coordination is likely to be rate determining for carbolithiation reactions in which the only Lewis bases present are either weakly donating (such as diethyl ether) or sufficiently sterically hindered (such as sparteine)⁷² that they are unable to cleave the alkylolithium clusters to monomers.^{67,68}

CONCLUDING REMARKS

In the solid state, the ω -alkenyllithium compound (2,2-dimethylpent-4-en-1-yl)lithium (**2**) is tetrameric and exhibits lithium–olefin π interactions, with average Li–C distances of 2.46(2) and 2.55(3) Å for the olefinic methine and methylene carbon atoms, respectively. In hydrocarbon solvents, **2** and its butenyl analog (2,2-dimethylbut-3-en-1-yl)lithium (**1**) remain tetrameric, and the lithium–olefin interactions are still present, as judged by DOSY and NOE measurements. VT-NMR and NOE studies in hydrocarbon solvents show that the lithium–olefin interactions persist in the presence of small amounts of diethyl ether, but are largely displaced by THF.

Deuterium labeling experiments reveal that the α -CH₂ and γ -CH₂ groups in the pentenyl compound **2** can exchange with one another, showing that this compound can undergo reversible intramolecular carbolithiation via a higher energy (and unobservable) cyclobutylmethyl intermediate. Interestingly, however, the rate of this exchange process is highly solvent dependent. At –20 °C in hydrocarbon solvents, the process is very slow (no detectable exchange after 7 days), but in 1:1 pentane/diethyl ether, the deuterium labels become fully equilibrated over the two sites after several days.

Addition of a Lewis base such as THF to these ω -alkenyllithium species has two effects: the THF displaces the lithium–olefin interactions while accelerating the rate of carbolithiation. This situation is interesting, because coordination of the olefin to the lithium is needed for carbolithiation to occur. It has generally been assumed that the C–C bond formation step in carbolithiation reactions is rate determining, but we suggest that coordination of the olefin to lithium (perhaps also inducing disaggregation of the lithium clusters to form monomeric species) may be rate determining in some systems. We propose that this will be the case when the only Lewis bases present are either weakly donating (such as diethyl ether) or sterically hindered (such as sparteine).

EXPERIMENTAL SECTION

All experiments were carried out in a vacuum or under argon using standard Schlenk techniques. All glassware was oven-dried before use. Solvents (pentane, diethyl ether) were distilled under nitrogen from sodium/benzophenone immediately before use. Lithium granules (4–10 mesh, trace metals grade, Sigma-Aldrich) were used as received. Cyclohexane-*d*₁₂, benzene-*d*₆, methylcyclohexane-*d*₁₄, and chloroform-*d*₁ were purchased from Sigma-Aldrich or Cambridge Isotope Laboratories in 1 mL ampules and used without purification. The compounds 5-bromo-4,4-dimethyl-1-pentene⁷⁴ and 6-bromo-5,5-dimethyl-1-hexene^{75,76} were prepared by slightly modified literature routes as described in the SI. The syntheses of 4-bromo-3,3-dimethyl-1-butene and 5,5-*d*₂-5-bromo-4,4-dimethyl-1-pentene are reported in detail in the SI.

Elemental analyses were performed by the University of Illinois Microanalytical Laboratory. In order to obtain satisfactory CHN combustion analyses, it was necessary to add a combustion aid (a mixture of silver vanadate, silver tungstate, and cobaltic oxide), so as to avoid formation of Li₂CO₃, which is known to retain CO₂ tenaciously.⁷⁷ FTIR spectra were acquired on a Thermo Nicolet IR200 spectrometer as mineral oil mulls between KBr plates, and processed using the OMNIC software package with automatic baseline corrections. Melting points were acquired on a Thomas-Hoover Uni-Melt apparatus in sealed capillaries under argon. The 1D ¹H and ¹³C NMR data were recorded on a Varian Inova 400 spectrometer at 9.39 T or Varian Inova 500 spectrometer at 11.74 T. The ¹H–¹H NOE data were recorded on a Varian Inova 500 spectrometer at 11.74 T or Varian Inova 600 spectrometer at 14.09 T. ¹H DOSY data were recorded on an Agilent VNMRS NMR 750 spectrometer at 17.61 T. The ⁷Li NMR and ⁷Li–¹H 1D NOE data were recorded on a Varian Inova 600 spectrometer at 14.09 T. Chemical shifts are reported in δ units (positive shifts to higher frequency) relative to TMS (¹H, ¹³C), set by assigning appropriate shifts to residual solvent signals, or to an external standard of aqueous 1.0 M LiCl (⁷Li) by sample replacement. Because the alkylolithium compounds are pyrophoric, PTFE liners (Wilmad) were placed inside the NMR tubes to prevent escape of the material in case of breakage. X-ray crystallographic data were collected by staff at the G. L. Clark X-ray Laboratory at the University of Illinois.

Caution: The following organolithium reagents are pyrophoric in air and react violently with water. Use proper safety precautions.

(2,2-Dimethylbut-3-en-1-yl)lithium (1). Krytox grease was used to lubricate all glass joints (see below). Lithium granules (4–10 mesh, trace metals grade, 3.0 g, 430 mmol) were dispersed in pentane (20 mL) with a glass-coated stirring bar; 4-bromo-3,3-dimethyl-1-butene (6.0 g, 37 mmol) was added, and the mixture was left stirring at room temperature for 12 h. Diethyl ether (20 mL) was then added at –20 °C, and the mixture was stirred at this temperature for 12 h. The solvent was removed at –20 °C, and the resulting solid was extracted with pentane (2 × 20 mL) to give a light yellow solution of product (40 mL of a 0.22 M solution, 29%). Evaporation of the solvent gives the title compound as a light yellow oil. ¹H NMR (500 MHz, C₆D₁₂, 20 °C): δ 6.07 (dd, 1 H, ³J_{HH} = 17.9, 10.6 Hz, =CH=), 4.95 (dd, 1 H, ³J_{HH} = 17.9 Hz, ²J_{HH} = 1.7 Hz, =CH₂), 4.84 (dd, 1 H, ³J_{HH} = 10.6 Hz, ²J_{HH} = 1.7 Hz, =CH₂), 1.07 (s, 6 H, Me), –0.80 (br, 2 H, Li–CH₂). ¹³C{¹H} NMR (126 MHz, C₆D₆, 20 °C): 155.01 (s, =CH=), 106.61 (s, =CH₂), 39.23 (s, 2-C), 33.87 (s, Me), 26.51 (br, Li–CH₂). ⁷Li NMR (233 MHz, C₆D₁₂, 20 °C): 2.01 (s).

Note: (2,2-Dimethylbut-3-en-1-yl)lithium reacts with silicone grease to form a dark oil that contains (2,2-dimethylbut-3-en-1-yl)dimethylsilanol, which has the following NMR properties. ¹H NMR (400 MHz, C₆D₆, 20 °C): δ 5.87 (dd, 1 H, ³J_{HH} = 8.8, 17.6 Hz, =CH=), 4.91 (dd, 1 H, ³J_{HH} = 17.6 Hz, ²J_{HH} = 1.4 Hz, =CH₂), 4.82 (dd, 1 H, ³J_{HH} = 8.8 Hz, ²J_{HH} = 1.4 Hz, =CH₂), 1.08 (s, 6 H, CMe₂), 0.70 (s, 2 H, SiCH₂), 0.10 (s, 6 H, SiMe₂). MS (EI, *m/e*) calcd, 158.1; found, 158.1.

(2,2-Dimethylpent-4-en-1-yl)lithium (2). A 100 mL Schlenk flask was charged with a glass-coated stirring bar, lithium granules (4–10 mesh, trace metals grade, 3.0 g, 432 mmol), pentane (30 mL), and

5-bromo-4,4-dimethyl-1-pentene (6.0 g, 34 mmol); the latter was added in one portion. The mixture was stirred for 24 h at room temperature and then was cooled to -20°C and diluted by slow addition of diethyl ether (30 mL). The mixture was stirred at -20°C for 10 h, and then the solvent was removed at -20°C . The residue was extracted with pentane (2×25 mL). The yellow extract was filtered, concentrated to ca. 3 mL, and cooled to -78°C . The off-white solid was collected and washed with cold pentane (2×2 mL). A second crop can be obtained by concentrating the mother liquor and cooling to -78°C . Combined yield: 2.28 g (65%). Anal. Calcd for $\text{C}_7\text{H}_{13}\text{Li}$: C, 80.7; H, 12.8. Found: C, 80.6; H, 12.4. Mp. 60–61 $^{\circ}\text{C}$. IR (cm^{-1}): 1628 (m, C=C stretch). ^1H NMR (500 MHz, C_6D_{12} , 20 $^{\circ}\text{C}$): δ 6.19 (m, 1 H, $-\text{CH}=\text{}$), 5.17 (d, 1 H, $^3J_{\text{HH}} = 17.4$ Hz, $=\text{CH}_2$), 5.11 (d, 1 H, $^3J_{\text{HH}} = 10.0$ Hz, $=\text{CH}_2$), 2.04 (d, 2 H, $^3J_{\text{HH}} = 7.4$ Hz, 3- CH_2), 1.06 (s, 6 H, Me), -0.83 (br s, 2 H, Li- CH_2). $^{13}\text{C}\{^1\text{H}\}$ NMR (126 MHz, C_6D_{12} , 20 $^{\circ}\text{C}$): δ 142.92 (s, $-\text{CH}=\text{}$), 116.87 (s, $=\text{CH}_2$), 52.80 (s, 3- CH_2), 38.81 (s, 2-C), 36.17 (s, Me), 32.71 (br s, Li- CH_2). ^7Li NMR (233 MHz, C_6D_{12} , 20 $^{\circ}\text{C}$): 2.01 (s).

^1H NMR (500 MHz, C_6D_6 , 20 $^{\circ}\text{C}$): δ 6.20 (m, 1 H, $-\text{CH}=\text{}$), 5.20 (d, 1 H, $^3J_{\text{HH}} = 17.4$ Hz, $=\text{CH}_2$), 5.11 (d, 1 H, $^3J_{\text{HH}} = 10.0$ Hz, $=\text{CH}_2$), 2.09 (d, 2 H, $^3J_{\text{HH}} = 7.4$ Hz, 3- CH_2), 1.19 (s, 6 H, Me), -0.71 (br s, 2 H, Li- CH_2). Small amounts of the hydrolysis product 4,4-dimethyl-1-pentene are present in the NMR sample: ^1H NMR (500 MHz, C_6D_6 , 20 $^{\circ}\text{C}$): δ 5.79 (m, 1 H, $-\text{CH}=\text{}$), 4.97–5.06 (m, 2 H, $=\text{CH}_2$), 1.87 (d, 2 H, $^3J_{\text{HH}} = 7.5$ Hz, 3- CH_2), 0.85 (s, 9 H, Me).

Compound 2 has previously been generated *in situ* from *tert*-butyl lithium and 5-iodo-4,4-dimethyl-1-pentene,⁷⁸ but was not isolated or characterized.

[(3,3-Dimethylcyclopentyl)methyl]lithium (3). The reaction of 6-bromo-5,5-dimethyl-1-hexene with lithium under the same conditions as those for the synthesis of **1** and **2** leads to a light-yellow product that shows no olefinic signals in the ^1H NMR spectrum. This product was identified as [(3,3-dimethylcyclopentyl)methyl]lithium. The product is an oil, which prevented us from determining an accurate yield by weighing; NMR studies suggest that the yield is approximately 80%. ^1H NMR (500 MHz, C_6D_6 , 20 $^{\circ}\text{C}$): δ 2.27 (m, 1 H), 2.09 (m, 1 H), 2.01 (dd, $^2J_{\text{HH}} = 11.8$ Hz, $^3J_{\text{HH}} = 10.2$ Hz, 1 H, CH_2), 1.66 (m, 1 H), 1.42 (m, 1 H), 1.53 (m, 1 H), 1.19 (dd, $^2J_{\text{HH}} = 11.8$ Hz, $^3J_{\text{HH}} = 6.8$ Hz, 1 H, CH_2), 1.15 (s, 3 H, Me), 1.11 (s, 3 H, Me), -0.60 (br, 2 H, Li- CH_2).

(1,1-d₂-2,2-Dimethylpent-4-en-1-yl)lithium (2- α -d₂). This compound was prepared from methyl 5,5-d-bromo-4,4-dimethyl-1-pentene (1.0 g, 5.6 mmol) by the same procedure for synthesizing the undeuterated analog. The product was obtained as a light yellow solution in pentane (27 mL of a 0.18 M solution, 88%). Evaporation of the solvent gives the title compound as a light yellow oil. ^1H NMR (500 MHz, C_6D_{12} , 20 $^{\circ}\text{C}$): δ 6.18 (m, 1 H, $-\text{CH}=\text{}$), 5.16 (d, 1 H, $^3J_{\text{HH}} = 10.0$ Hz, $=\text{CH}_2$), 5.10 (d, 1 H, $^3J_{\text{HH}} = 17.3$ Hz, $=\text{CH}_2$), 2.04 (d, 1.7 H, $^3J_{\text{HH}} = 7.4$ Hz, 3- CH_2), 1.05 (s, 6 H, Me), -0.83 (br s, 0.3 H, Li- CH_2). $^2\text{H}\{^1\text{H}\}$ NMR (77 MHz, C_6H_{12} , 20 $^{\circ}\text{C}$): 1.95 (s, 3- d_2), -0.91 (s, 1,1- d_2); integration ratio 4.7:1, corresponding to a 83:17 mixture of the 1,1- d_2 and 3,3- d_2 isotopologs, respectively.

Crystallographic Studies. Single crystals of (2,2-dimethylpent-4-en-1-yl)lithium (**2**), grown from pentane at -78°C , were difficult to mount because they are highly air and moisture sensitive and they quickly redissolve in the mother liquor when warmed to room temperature. With the crystallization solution kept at -78°C , most of the mother liquor was removed by cannula, and then the crystals were covered with Krytox 100 oil (DuPont) that had previously been degassed and cooled to -20°C . A suitable crystal was identified, transferred to a glass fiber, and immediately cooled to -173°C in a cold nitrogen gas stream on the diffractometer. Standard peak search and indexing procedures gave rough cell dimensions, and least-squares refinement using 22 137 reflections yielded the cell dimensions given in Table 1.

Data were collected with an area detector by using the measurement parameters listed in Table 1. The triclinic lattice and the average values of the normalized structure factors suggested the space group $\text{P}\bar{1}$, which was confirmed by the success of the subsequent refinement. The measured intensities were reduced to

structure factor amplitudes and their estimated standard deviations by correction for background, scan speed, and Lorentz and polarization effects. No corrections for crystal decay were necessary, but a face-indexed absorption correction was applied, the minimum and maximum transmission factors being 0.9706 and 1.0000. Systematically absent reflections were deleted, and symmetry equivalent reflections were averaged to yield the set of unique data. Two reflections, 0 2 2 and $-1\ 0\ 2$, were obscured by the beam stop and were deleted; the remaining 5504 unique data were used in the least-squares refinement.

Intensity data were collected on a Bruker D8 Venture kappa diffractometer equipped with a Photon 100 CMOS detector. An $\text{I}\mu\text{s}$ microfocus source provided the $\text{Mo K}\alpha$ radiation ($\lambda = 0.71073$ Å) that was monochromated with multilayer mirrors. The collection, cell refinement, and integration of intensity data were carried out with the APEX3 software.⁷⁹ Face-indexed absorption corrections were performed numerically with SADABS.⁸⁰ The initial structure solution was solved with direct methods SHELXS⁸¹ and refined with the full-matrix least-squares SHELXL⁸¹ program. The structure was solved by direct methods. Correct positions for all the non-hydrogen atoms were deduced from an E-map. Subsequent least-squares refinement and difference Fourier calculations revealed the positions of the hydrogen atoms. The quantity minimized by the least-squares program was $\sum w(F_0^2 - F_c^2)^2$, where $w = \{[\sigma(F_0^2)]^2 + (0.0543P)^2 + 1.181P\}^{-1}$ and $P = (F_0^2 + 2F_c^2)/3$. The analytical approximations to the scattering factors were used, and all structure factors were corrected for both real and imaginary components of anomalous dispersion. In the final cycle of least-squares, independent anisotropic displacement factors were refined for the non-hydrogen atoms. Methyl hydrogen atoms were placed in idealized positions; the rest of hydrogen atoms were located in the difference maps. The methyl groups were allowed to rotate about the C–C axis to find the best least-squares positions. The displacement parameters for methylene and methine hydrogens were set equal to 1.2 times U_{eq} for the attached carbon; those for methyl hydrogens were set to 1.5 times U_{eq} . An isotropic extinction parameter was refined to a final value of $x = 1.17(6) \times 10^{-4}$ where F_c is multiplied by the factor $k[1 + F_c^2 x \lambda^3 / \sin 2\theta]^{-1/4}$ with k being the overall scale factor. Successful convergence was indicated by the maximum shift/error of 0.001 for the last cycle. Final refinement parameters are given in Table 1. The largest peak in the final Fourier difference map (0.77 e/Å³) was located 0.93 Å from C31 (lone pair electrons). A final analysis of variance between observed and calculated structure factors showed no apparent errors.

DOSY Experiments. DOSY experiments were performed on an Agilent VNMRS 750 spectrometer capable of performing pulsed field gradient (PFG) spin-echo diffusion measurements. Solutions of **1** or **2** (~15 mM) in C_6D_{12} were prepared in oven-dried NMR tubes, which were then flame-sealed. The sample of **2** also contained adamantane (~15 mM) as a diffusion standard. The solutions were thermally equilibrated for ~30 min in the probe at 25 $^{\circ}\text{C}$ before data collection. Diffusion experiments were performed by means of a DOSY gradient compensated stimulated echo with a spin lock and convection compensation sequence (DgsteSL_cc)⁸² with a 2 ms trim pulse, a spectral width of 7485 Hz, a diffusion gradient time of 2 ms, a diffusion delay of 50.0 ms, and 16 gradient levels in the range 2.79–60.03 G/cm. The data were processed with the VNMR J4.2A software. The baselines of all spectra were corrected before data processing.

Molecular weights were determined from reported external calibration curves using adamantane as the internal standard:⁵¹ the NMR-measured diffusivity, D_x , is first converted to a normalized diffusivity, $D_{x,\text{norm}}$, that corrects for various factors (such as temperature, convective motion, solvent viscosity, solute concentrations, and NMR parameters such as gradient strength and pulse durations) that are known to influence measured diffusivities. We performed this correction by making use of the equation $\log D_{x,\text{norm}} = -9.0204 - \log D_{\text{adam}} + \log D_x$ where D_{adam} is the measured diffusion coefficient of a calibration standard, adamantane, under our experimental conditions ($(7.53 \pm 0.02) \times 10^{-10}$ m²/s).^{50,51} The normalized diffusion coefficient was then used to estimate the

molecular weights of our organolithium compounds in solution by means of the equation $\log D_{x,\text{norm}} = \log K + \alpha MW$, where the values $\log K = -7.62$ and $\alpha = -0.620$, respectively, are obtained from reported calibrations of different solutes in C_6D_{12} at 25 °C; the estimated accuracy of the resulting molecular weight is typically $\pm 15\%$.⁵¹

NOE NMR Experiments. NOE experiments were performed at room temperature (25 °C) on solutions of **1** and **2** (0.24 M) in C_6D_{12} placed in flame-sealed NMR tubes. The ^7Li – ^1H NOE difference spectrum was obtained by subtracting a standard ^1H spectrum from the ^1H spectrum collected after saturating the ^7Li resonance for 5 s, with a recycle delay of 2.0 s. The ^1H 1D NOE NMR spectrum was measured by means of a Cyclenoe experiment with a 2.0 s saturation time. NOE experiments on **2** in the presence of diethyl ether and THF were performed using the same parameters at –38.1 °C to avoid deprotonation of the ether molecules.⁸³

Estimation of ΔH^\ddagger for a Two-Site Exchange Process from NMR Line Shape Analysis above the Coalescence Temperature. The line width of the 2-Me resonance in the pentenyllithium compound **2** increases as the temperature is lowered (see SI), owing to the onset of a decoalescence process in which the rate of dissociation of the C=C bond from the Li center is changing from fast to slow on the NMR time scale. For an exchange process between two sites of equal population, as in the present case, the line width of the coalesced peak in the fast exchange regime (i.e., above the coalescence temperature) is approximately related to the rate of exchange by the equation:

$$k = \frac{\pi \Delta\nu_{AB}^2}{2(\Delta\nu - \Delta\nu_{\text{ref}})}$$

where $\Delta\nu_{AB}$ is the chemical shift difference between the two exchanging sites, $\Delta\nu$ is the full width at half-maximum (fwhm) of the coalesced singlet, and $\Delta\nu_{\text{ref}}$ is the fwhm of a nonexchanging reference singlet.⁸⁴ If $\Delta\nu_{AB}$ is unknown (which is true for dissociation of the C=C bond from lithium in **2** because even the lowest temperature examined was above the coalescence point for the 2-Me groups), the absolute exchange rate cannot be calculated from the line widths in the fast exchange regime. We point out, however, that the relative rates of exchange as a function of temperature can be determined from the line widths, and from this information we can deduce the enthalpy of activation for the exchange process. The analysis proceeds as follows.

Let us define $1/2 \pi \Delta\nu_{AB}^2$ as the constant A , and let $1/(\Delta\nu - \Delta\nu_{\text{ref}})$ be represented by D , so that $k = AD$. Now, D can be measured, but A is unknown so we do not know the absolute rate. But changes in D as the sample is warmed or cooled will give us information about the relative rates as a function of temperature.

The Eyring equation, expressed in logarithmic form, is

$$\ln(k/T) = \ln(k_B/h) - \Delta H^\ddagger/RT + \Delta S^\ddagger/R$$

Substituting $k = AD$ and rearranging gives

$$\ln(D/T) = [\ln(k_B/h) + \Delta S^\ddagger/R - \ln A] - \Delta H^\ddagger/RT$$

Because A is a constant, the quantity in the brackets is also a constant, and ΔH^\ddagger can be derived from the slope of a plot $\ln(D/T)$ versus $1/T$. If line shape data are available only above the coalescence temperature (as in the present case), then A is unknown and the value of ΔS^\ddagger cannot be determined.

The line width of the 4-methyl resonance of the hydrolysis product 4,4-dimethyl-1-pentene broadens slightly as the temperature is lowered, probably due to instrumental or solvent viscosity effects. If we use the line width at this peak at each temperature as $\Delta\nu_{\text{ref}}$, then a plot $\ln(D/T)$ versus $1/T$ for the 2-Me resonance of **2** gives a value for the activation enthalpy for C=C bond dissociation, ΔH^\ddagger , of 2.1 kcal/mol. Alternatively, because the line width of the 2-Me resonance of **2** changes very little between –10 to –30 °C, we can assume that at –10 °C the 2-Me resonance of **2** is in the fast-exchange limit; at this temperature, the line width of this resonance is 1.15 Hz larger than the line width of the Me resonance of the hydrolysis product. If we

assume that the natural line width of the 2-Me resonance of **2** is 1.15 Hz larger than the line width of the Me resonance of the hydrolysis product at all temperatures, then a plot $\ln(D/T)$ versus $1/T$ for the 2-Me resonance of **2** gives a value for the activation enthalpy for C=C bond dissociation, ΔH^\ddagger , of 3.6 kcal/mol.

ASSOCIATED CONTENT

Supporting Information

The Supporting Information is available free of charge on the ACS Publications website at DOI: 10.1021/acs.organomet.9b00169.

Synthesis and characterization of intermediates for the synthesis of 4-bromo-3,3-dimethyl-1-butene, 5-bromo-4,4-dimethyl-1-pentene, 6-bromo-5,5-dimethyl-1-hexene, and 5,5- d_2 -5-bromo-4,4-dimethyl-1-pentene; a list of complete bond lengths and angles for **2**; room temperature ^1H , ^{13}C , ^2H , and ^7Li NMR spectra of the alkylolithium compounds and selected synthetic intermediates; IR spectrum of **2**; DOSY spectrum for **1** and ^1H – ^1H NOE and ^7Li – ^1H NOE spectra of **1** and **2**; spectroscopic evidence for the reversible carbolithiation of **2**; variable temperature ^1H NMR spectra of **2** in toluene- d_8 , including a list of line widths of selected resonances and calculation of ΔH^\ddagger for C=C bond dissociation; ^1H NMR, ^7Li NMR, ^1H – ^1H NOE, ^7Li – ^1H NOE spectra and a list of NOEs and chemical shifts of selected resonances of **2** at –38.1 °C in the presence of coordinating molecules (PDF)

Accession Codes

CCDC 1909998 contains the supplementary crystallographic data for this paper. These data can be obtained free of charge via www.ccdc.cam.ac.uk/data_request/cif, or by emailing data_request@ccdc.cam.ac.uk, or by contacting The Cambridge Crystallographic Data Centre, 12 Union Road, Cambridge CB2 1EZ, UK; fax: +44 1223 336033.

AUTHOR INFORMATION

Corresponding Author

*E-mail: girolami@scs.illinois.edu.

ORCID

Sumeng Liu: 0000-0002-2133-2122

Danielle Gray: 0000-0003-0059-2096

Gregory S. Girolami: 0000-0002-7295-1775

Notes

The authors declare no competing financial interest.

ACKNOWLEDGMENTS

The authors thank the National Science Foundation (CHE 1362931 and CHE 1665191) for support of this research. Dedicated to Professor Theodore L. Brown on the occasion of his 90th birthday.

REFERENCES

- (1) Minko, Y.; Marek, I. Advances in Carbolithiation. In *Lithium Compounds in Organic Synthesis: From Fundamentals to Applications*, 1st ed.; Luisi, R., Capriati, V., Eds.; Wiley-VCH: Weinheim, 2014; pp 329–350.
- (2) Gómez-SanJuan, A.; Sotomayor, N.; Lete, E. Inter- and Intramolecular Enantioselective Carbolithiation Reactions. *Beilstein J. Org. Chem.* 2013, 9, 313–322.

(3) Fañanás, F. J.; Sanz, R. Intramolecular Carbolithiation Reactions. In *The Chemistry of Organolithium Compounds*; Rappoport, Z., Marek, I., Eds.; John Wiley & Sons, Ltd.: New York, 2006; pp 295–379.

(4) Bailey, W. F.; Patricia, J. J.; DelGobbo, V. C.; Jarret, R. M.; Okarma, P. J. Cyclization of 5-Hexenyllithium to (Cyclopentylmethyl)lithium. *J. Org. Chem.* **1985**, *50*, 1999–2000.

(5) Reich, H. J. Role of Organolithium Aggregates and Mixed Aggregates in Organolithium Mechanisms. *Chem. Rev.* **2013**, *113*, 7130–7178.

(6) St. Denis, J.; Dolzine, T.; Oliver, J. P. Intramolecular Metal-Double Bond Interaction. III. Intramolecular Cyclization Reactions of Organometallic Compounds. *J. Am. Chem. Soc.* **1972**, *94*, 8260–8261.

(7) Bailey, W. F.; Punzalan, E. R. "Super Bases" Derived from 5-Hexenyllithium and Alkali Metal Alkoxides: Rearrangements of 5-Hexenylalkalis. *J. Am. Chem. Soc.* **1994**, *116*, 6577–6580.

(8) Bailey, W. F.; Jiang, X.-L.; McLeod, C. E. Conformational Control in the Cyclization of an Unsaturated Vinylolithium: Synthesis of (\pm)-Laurene. *J. Org. Chem.* **1995**, *60*, 7791–7795.

(9) Mattalia, J.-M.; Nava, P. A Computational Study of the Intramolecular Carbolithiation of Aryllithiums: Solvent and Substituent Effects. *Eur. J. Org. Chem.* **2016**, *2016*, 394–401.

(10) Bailey, W. F.; Mealy, M. J. Asymmetric Cyclization of Achiral Olefinic Organolithiums Controlled by a Stereogenic Lithium: Intramolecular Carbolithiation in the Presence of (–)-Sparteine. *J. Am. Chem. Soc.* **2000**, *122*, 6787–6788.

(11) Jutzi, P. π Bonding to Main-Group Elements. In *Advances in Organometallic Chemistry*; Stone, F. G. A., West, R., Eds.; Academic Press: 1986; Vol. 26, pp 217–295.

(12) Unkelbach, C.; Strohmann, C. Low-Temperature Addition of Organolithiums to Functionalized Vinylsilanes under Formation of Secondary α -Lithiated Alkylsilanes. *J. Am. Chem. Soc.* **2009**, *131*, 17044–17045.

(13) Hogan, A.-M. L.; O'Shea, D. F. Synthetic Applications of Carbolithiation Transformations. *Chem. Commun.* **2008**, 3839–3851.

(14) Suga, Y.; Oku, J.-i.; Masuda, H.; Takaki, M.; Mukai, M.; Kitagawa, T. Mechanism of the Anionic Cyclopolymerization of Bis(dimethylvinylsilyl)methane. *Macromolecules* **1999**, *32*, 1362–1366.

(15) Bailey, W. F.; Khanolkar, A. D.; Gavaskar, K.; Ovaska, T. V.; Rossi, K.; Thiel, Y.; Wiberg, K. B. Stereoselectivity of Cyclization of Substituted 5-Hexen-1-yllithiums: Regiospecific and Highly Stereoselective Insertion of an Unactivated Alkene into a Carbon-lithium bond. *J. Am. Chem. Soc.* **1991**, *113*, 5720–5727.

(16) Tomooka, K.; Komine, N.; Nakai, T. Cyclization of Enantio-enriched α -(Homoallyloxy)alkyllithiums: Evidence for Retention of Configuration at the Carbanion Center. *Tetrahedron Lett.* **1997**, *38*, 8939–8942.

(17) Woltering, M. J.; Fröhlich, R.; Hoppe, D. Synthesis of Enantiomerically and Diastereomerically Pure Cyclopentanols by Asymmetric Cyclocarbolithiation of 5-Alkenyl Carbamates. *Angew. Chem., Int. Ed. Engl.* **1997**, *36*, 1764–1766.

(18) Marek, I. Enantioselective Carbometallation of Unactivated Olefins. *J. Chem. Soc., Perkin Trans. 1* **1999**, 535–544.

(19) Houk, K. N.; Rondan, N. G.; Schleyer, P. v. R.; Kaufmann, E.; Clark, T. Transition Structures for Additions of Lithium Hydride and Methyllithium to Ethylene and Acetylene. *J. Am. Chem. Soc.* **1985**, *107*, 2821–2823.

(20) Liu, H.; Deng, K.; Cohen, T.; Jordan, K. D. Computational Study of the Stereochemistry of Intramolecular Carbolithiation of an Alkene by a Secondary Alkyllithium: Stereochemistry Change Caused by a Single THF Molecule of Solvation. *Org. Lett.* **2007**, *9*, 1911–1914.

(21) Bartlett, P. D.; Friedman, S.; Stiles, M. The Reaction of Isopropyllithium and t-Butyllithium with Simple Olefins. *J. Am. Chem. Soc.* **1953**, *75*, 1771–1772.

(22) Rolle, T.; Hoffmann, R. W. Direct Observation of an Internally π -Complexed Alkenyllithium Compound in THF solution. *J. Chem. Soc., Perkin Trans. 2* **1995**, 1953–1954.

(23) Hill, E. A.; Richey, H. G.; Ree, T. C. Intramolecular Cleavage and Double Bond Additions of Polar Organometallic Compounds. *J. Org. Chem.* **1963**, *28*, 2161–2164.

(24) Rodriguez, C.; Nudelman, N. S. Intramolecular Carbolithiation-Cyclization-Electrophilic Substitution: Solvent Effect and Mechanistic Study. *J. Phys. Org. Chem.* **2014**, *27*, 322–326.

(25) Smart, J. B.; Hogan, R.; Scherr, P. A.; Emerson, M. T.; Oliver, J. P. Metal-Double Bond Interactions: IV. A Study of Lithium- π -Electron Interactions in 3-Butenyllithium by 7 Li and 1 H NMR Spectroscopy. *J. Organomet. Chem.* **1974**, *64*, 1–17.

(26) Oliver, J. P.; Smart, J. B.; Emerson, M. T. Lithium- π -Electron Interactions in But-3-enyllithium. *J. Am. Chem. Soc.* **1966**, *88*, 4101–4103.

(27) Schiemenz, B.; Power, P. P. Synthesis and Structure of a Unique Monomeric σ -Bonded Aryllithium Compound Stabilized by a Weak Li-Benzene π Interaction. *Angew. Chem., Int. Ed. Engl.* **1996**, *35*, 2150–2152.

(28) Setzer, W. N.; Schleyer, P. V. R. X-Ray Structural Analyses of Organolithium Compounds. In *Advances in Organometallic Chemistry*; Stone, F. G. A., West, R., Eds.; Academic Press: New York, 1985; Vol. 24, pp 353–451.

(29) von Schleyer, P. R. Remarkable Structures of Lithium Compounds. *Pure Appl. Chem.* **1984**, *56*, 151–162.

(30) Klein, H. F.; Witty, H.; Schubert, U. The First Lithium Carrier in Hydrocarbons: Structure of LiCo(C₂H₄)(PMe₃)₃ Trimer. *J. Chem. Soc., Chem. Commun.* **1983**, 231–232.

(31) Deng, L.; Cheung, M.-S.; Chan, H.-S.; Xie, Z. Reduction of 1,2-(CH₂)_n-1,2-C₂B₁₀H₁₀ by Group 1 Metals. Effects of Bridge Length/Rigidity on the Formation of Carborane Anions. *Organometallics* **2005**, *24*, 6244–6249.

(32) Hertkorn, N.; Köhler, F. H.; Müller, G.; Reber, G. Bicyclo[3.2.1]octa-2,6-dienyllithium. *Angew. Chem., Int. Ed. Engl.* **1986**, *25*, 468–469.

(33) Negishi, E.; Swanson, D. R.; Rousset, C. J. Clean and Convenient Procedure for Converting Primary Alkyl Iodides and α,ω -Diiodoalkanes into the Corresponding Alkyllithium Derivatives by Treatment with tert-Butyllithium. *J. Org. Chem.* **1990**, *55*, 5406–5409.

(34) Hata, G. Aluminium-Olefinic Double Bond Interaction in Alkenylaluminium Compounds. *Chem. Commun.* **1968**, *0*, 7–9.

(35) Dolzine, T. W.; Oliver, J. P. Intramolecular Metal-Double Bond Interactions. VI. Metal- π -Electron Interactions Observed in Trialkenylaluminum and -gallium Derivatives. *J. Am. Chem. Soc.* **1974**, *96*, 1737–1740.

(36) Spectral Database for Organic Compounds (SDBS); IR spectrum; SDBS No.: 6020; RN 762–62–9; <http://sdbs.db.aist.go.jp/> (accessed June 9, 2018).

(37) Hartley, F. R. Olefin and Acetylene Complexes of Platinum and Palladium. *Chem. Rev.* **1969**, *69*, 799–844.

(38) Günther, H.; Moskau, D.; Bast, P.; Schmalz, D. Modern NMR Spectroscopy of Organolithium Compounds. *Angew. Chem., Int. Ed. Engl.* **1987**, *26*, 1212–1220.

(39) Mann, B. E.; Taylor, B. F. 13 C NMR Data for Organometallic Compounds; Academic Press: 1981.

(40) Gessner, V. H.; Däschlein, C.; Strohmann, C. Structure Formation Principles and Reactivity of Organolithium Compounds. *Chem. - Eur. J.* **2009**, *15*, 3320–3334.

(41) Klumpp, G. W.; Geurink, P. J. A.; Spek, A. L.; Duisenberg, A. J. M. X-Ray Crystal Structure of Tetrameric 3-Lithio-1-methoxybutane. *J. Chem. Soc., Chem. Commun.* **1983**, 814–816.

(42) Klumpp, G. W.; Vos, M.; De Kanter, F. J. J.; Slob, C.; Krabbendam, H.; Spek, A. L. X-ray Crystal Structure and Hydrocarbon Solution Dynamics of Tetrameric 1-(Dimethylamino)-3-lithiopropane. *J. Am. Chem. Soc.* **1985**, *107*, 8292–8294.

(43) Klumpp, G. W.; Geurink, P. J. A.; van Eikema Hommes, N. J. R.; de Kanter, F. J. J.; Vos, M.; Spek, A. L. X-Ray Structure of Tetrameric 1-Lithio-3-methoxypropane. *Recl. Trav. Chim. Pays-Bas* **1986**, *105*, 398–403.

(44) Cordero, B.; Gómez, V.; Platero-Prats, A. E.; Revés, M.; Echeverría, J.; Cremades, E.; Barragán, F.; Alvarez, S. Covalent Radii Revisited. *Dalton Trans.* **2008**, 2832–2838.

(45) Mantina, M.; Chamberlin, A. C.; Valero, R.; Cramer, C. J.; Truhlar, D. G. Consistent van der Waals Radii for the Whole Main Group. *J. Phys. Chem. A* **2009**, 113, 5806–5812.

(46) Allen, F. H.; Kennard, O.; Watson, D. G.; Brammer, L.; Orpen, A. G.; Taylor, R. Tables of Bond Lengths Determined by X-ray and Neutron Diffraction. Part 1. Bond Lengths in Organic Compounds. *J. Chem. Soc., Perkin Trans. 2* **1987**, S1–S19.

(47) Schumann, H.; Schutte, S.; Kroth, H.-J.; Lentz, D. Butenyl-Substituted Alkaline-Earth Metallocenes: A First Step towards Olefin Complexes of the Alkaline-Earth Metals. *Angew. Chem., Int. Ed.* **2004**, 43, 6208–6211.

(48) Schnöckel, H.; Leimkühler, M.; Lotz, R.; Mattes, R. Dimeric 1,4-Dichloro-2,3,5,6-tetramethyl-1,4-dialumina-2,5-cyclohexadiene, a Compound with Aluminum-Olefin π -Bonds. *Angew. Chem., Int. Ed. Engl.* **1986**, 25, 921–922.

(49) Carpentier, J.-F.; Wu, Z.; Lee, C. W.; Strömberg, S.; Christopher, J. N.; Jordan, R. F. d^0 Metal Olefin Complexes. Synthesis, Structures, and Dynamic Properties of $(C_5R_5)_2Zr(OCMe_2CH_2CH_2CH_2)^+$ Complexes: Models for the Elusive $(C_5R_5)_2Zr(R)(Olefin)^+$ Intermediates in Metallocene-Based Olefin Polymerization Catalysis. *J. Am. Chem. Soc.* **2000**, 122, 7750–7767.

(50) Neufeld, R.; Stalke, D. Accurate Molecular Weight Determination of Small Molecules via DOSY-NMR by Using External Calibration Curves with Normalized Diffusion Coefficients. *Chem. Sci.* **2015**, 6, 3354–3364.

(51) Bachmann, S.; Neufeld, R.; Dzemski, M.; Stalke, D. New External Calibration Curves (ECCs) for the Estimation of Molecular Weights in Various Common NMR Solvents. *Chem. - Eur. J.* **2016**, 22, 8462–8465.

(52) Windsor, C. G.; Saunderson, D. H.; Sherwood, J. N.; Taylor, D.; Pawley, G. S. Lattice Dynamics of Adamantane in the Disordered Phase. *J. Phys. C: Solid State Phys.* **1978**, 11, 1741.

(53) Thomas, R. D.; Jensen, R. M.; Young, T. C. Aggregation States and Exchange Properties of Alkyllithium Compounds in Hydrocarbon Solvent from ^{13}C - 6Li Coupling. *Organometallics* **1987**, 6, 565–571.

(54) Lewis, H. L.; Brown, T. L. Association of Alkyllithium Compounds in Hydrocarbon Media. Alkyllithium-Base Interactions. *J. Am. Chem. Soc.* **1970**, 92, 4664–4670.

(55) Su, C.; Hopson, R.; Williard, P. G. Characterization of Cyclopentyllithium and Cyclopentyllithium Tetrahydrofuran Complex. *J. Am. Chem. Soc.* **2013**, 135, 12400–12406.

(56) Geurink, P. J. A.; Klumpp, G. W. Enthalpies of Intramolecular Etheration of Saturated Organolithium Compounds in Benzene. *J. Am. Chem. Soc.* **1986**, 108, 538–539.

(57) Carpentier, J.-F.; Maryin, V. P.; Luci, J.; Jordan, R. F. Solution Structures and Dynamic Properties of Chelated d^0 Metal Olefin Complexes $\{\eta^5: \eta^1-C_5R_4SiMe_2N^tBu\}Ti(OCMe_2CH_2CH_2CH_2)^+$ ($R = H, Me$): Models for the $\{\eta^5: \eta^1-CSR_4SiMe_2N^tBu\}Ti(R')(Olefin)^+$ Intermediates in “Constrained Geometry” Catalysts. *J. Am. Chem. Soc.* **2001**, 123, 898–909.

(58) Casey, C. P.; Hallenbeck, S. L.; Wright, J. M.; Landis, C. R. Formation and Spectroscopic Characterization of Chelated d^0 Yttrium(III)-Alkyl-Alkene Complexes. *J. Am. Chem. Soc.* **1997**, 119, 9680–9690.

(59) Quirk, R. P.; Kester, D. E. Solvation of Alkyllithium Compounds. Steric Effects on Heats of Interaction of Bases with Hexameric versus Tetrameric Alkyllithiums. *J. Organomet. Chem.* **1977**, 127, 111–125.

(60) Hill, E. A.; Ni, H.-R. Rearrangement of the Grignard Reagent from 5-Chloro-1-pentene-5, d_2 . *J. Org. Chem.* **1971**, 36, 4133–4134.

(61) Baldwin, J. E. Rules for Ring Closure. *J. Chem. Soc., Chem. Commun.* **1976**, 734–736.

(62) Gilmore, K.; Mohamed, R. K.; Alabugin, I. V. The Baldwin Rules: Revised and Extended. *WIREs Comput. Mol. Sci.* **2016**, 6, 487–514.

(63) Lewis, G. N.; Randall, M.; Pitzer, K. S.; Brewer, L. *Thermodynamics*. 2nd ed.; McGraw-Hill: New York, 1962; p 163.

(64) Bailey, W. F.; Rossi, K. Tandem Anionic Cyclization Approach to Polycarbocyclic Products. *J. Am. Chem. Soc.* **1989**, 111, 765–766.

(65) Wakefield, B. J. Addition of Organolithium Compounds to Carbon–Carbon Multiple Bonds. In *The Chemistry of Organolithium Compounds*, 1st ed.; Wakefield, B. J., Ed.; Pergamon: 1974; pp 89–108.

(66) Reich, H. J.; Green, D. P.; Medina, M. A.; Goldenberg, W. S.; Gudmundsson, B. Ö.; Dykstra, R. R.; Phillips, N. H. Aggregation and Reactivity of Phenyllithium Solutions. *J. Am. Chem. Soc.* **1998**, 120, 7201–7210.

(67) Sott, R.; Håkansson, M.; Hilmersson, G. Studies of Complexes between Phenyllithium and (–)-Sparteine in Ether Solutions. *Organometallics* **2006**, 25, 6047–6053.

(68) Carbone, G.; O’Brien, P.; Hilmersson, G. Asymmetric Deprotonation using *s*-BuLi or *i*-PrLi and Chiral Diamines in THF: The Diamine Matters. *J. Am. Chem. Soc.* **2010**, 132, 15445–15450.

(69) Owen, J. S.; Labinger, J. A.; Bercaw, J. E. Kinetics and Mechanism of Methane, Methanol, and Dimethyl Ether C–H Activation with Electrophilic Platinum Complexes. *J. Am. Chem. Soc.* **2006**, 128, 2005–2016.

(70) Chen, G. S.; Labinger, J. A.; Bercaw, J. E. The Role of Alkane Coordination in C–H Bond Cleavage at a Pt(II) center. *Proc. Natl. Acad. Sci. U. S. A.* **2007**, 104, 6915.

(71) Zhong, H. A.; Labinger, J. A.; Bercaw, J. E. C–H Bond Activation by Cationic Platinum(II) Complexes: Ligand Electronic and Steric Effects. *J. Am. Chem. Soc.* **2002**, 124, 1378–1399.

(72) Gil, G. S.; Groth, U. M. Enantioselective Synthesis of 3-Substituted Indolines by Asymmetric Intramolecular Carbolithiation in the Presence of (–)-Sparteine. *J. Am. Chem. Soc.* **2000**, 122, 6789–6790.

(73) Darensbourg, M. Y.; Kimura, B. Y.; Hartwell, G. E.; Brown, T. L. Cross-Association of *t*-Butyllithium. Kinetics of *t*-Butyllithium Dissociation. *J. Am. Chem. Soc.* **1970**, 92, 1236–1242.

(74) Briniouille, R.; Guo, H.; Bach, T. Enantioselective Intramolecular [2 + 2] Photocycloaddition Reactions of 4-Substituted Coumarins Catalyzed by a Chiral Lewis Acid. *Chem. - Eur. J.* **2012**, 18, 7552–7560.

(75) Ashby, E. C.; Park, B.; Patil, G. S.; Gadru, K.; Gurumurthy, R. Competing Radical, Carbanion, and Carbene Pathways in the Reactions of Hindered Primary Alkyl Halides with Lithium Dialkylamides. *J. Org. Chem.* **1993**, 58, 424–437.

(76) Hoye, T. R.; Van Veidhuizen, J. J.; Vos, T. J.; Zhao, P. A Useful Modification of the Kraus Procedure for Preparation of ω -Bromo-1-alkenes by HMPA-Promoted Elimination of HBr from 1, ω -Dibromoalkanes. *Synth. Commun.* **2001**, 31, 1367–1371.

(77) Timoshevskii, A. N.; Ktalkherman, M. G.; Emel’kin, V. A.; Pozdnyakov, B. A.; Zamyatin, A. P. High-temperature Decomposition of Lithium Carbonate at Atmospheric Pressure. *High Temp.* **2008**, 46, 414–421.

(78) Weatherhead, G. S.; Cortez, G. A.; Schrock, R. R.; Hoveyda, A. H. Mo-catalyzed asymmetric olefin metathesis in target-oriented synthesis: Enantioselective synthesis of (+)-africanol. *Proc. Natl. Acad. Sci. U. S. A.* **2004**, 101, 5805.

(79) APEX3; Bruker AXS, Inc.: Madison, Wisconsin, USA, 2018.

(80) Krause, L.; Herbst-Irmer, R.; Sheldrick, G. M.; Stalke, D. Comparison of silver and molybdenum microfocus X-ray sources for single-crystal structure determination. *J. Appl. Crystallogr.* **2015**, 48, 3–10.

(81) Sheldrick, G. Crystal structure refinement with SHELXL. *Acta Crystallogr., Sect. C: Struct. Chem.* **2015**, 71, 3–8.

(82) Jerschow, A.; Müller, N. Suppression of Convection Artifacts in Stimulated-Echo Diffusion Experiments. Double-Stimulated-Echo Experiments. *J. Magn. Reson.* **1997**, 125, 372–375.

(83) Totter, F.; Rittmeyer, P. Organolithium Compounds — Industrial Applications and Handling. In *Organometallics in Synthesis*; Schlosser, M., Ed.; John Wiley & Sons Ltd.: New York, 2013; pp 168–194.

(84) Binsch, G. Band-Shape Analysis. In *Dynamic Nuclear Magnetic Resonance Spectroscopy*; Jackman, L. M., Cotton, F. A., Eds.; Academic Press: Cambridge, 1975; pp 45–81.